Delft University of Technology

Sodium silicate/polyurethane microcapsules synthesized for enhancing self-healing ability of cementitious materials
Optimization of stirring speeds and evaluation of self-healing efficiency

Beglarigale, Ahsanollah; Eyice, Doğa ; Seki, Yoldaş ; Yalçinkaya, Çağlar; Copuroglu, Oguzhan; Yazici, Halit

Important note
To cite this publication, please use the final published version (if applicable).
Please check the document version above.

Sodium silicate/polyurethane microcapsules synthesized for enhancing self-healing ability of cementitious materials: Optimization of stirring speeds and evaluation of self-healing efficiency

Ahsanollah Beglarigale [a, *], Doğa Eyice [b], Yoldaş Seki [c], Çağlar Yalçınkaya [b,d], Oğuzhan Çopuroğlu [d], Halit Yazıcı [b]

[a] *Department of Civil Engineering, Istanbul Okan University, Tuzla, Istanbul, Turkey*
[b] *Department of Civil Engineering, Dokuz Eylül University, Buca, İzmir, Turkey*
[c] *Department of Chemistry, Dokuz Eylül University, Buca, İzmir, Turkey*
[d] *Faculty of Civil Engineering and Geosciences, Section Materials & Environment, Delft University of Technology, 2628, CN, Delft, the Netherlands*

ARTICLE INFO

ABSTRACT

In this study, stirring speeds during the synthesizing process of the sodium silicate/polyurethane microcapsules were optimized. The yield values of microcapsules at different stirring rates were evaluated. Based on the yield values and shape of microcapsules, optimized microcapsules were obtained. The measurements of the shell thickness of microcapsules were performed on the fractured microcapsules by using scanning electron microscopy. The optimized microcapsules were further characterized by means of optical microscopy and nano-indentation. Load vs. displacement and modulus of elasticity vs. displacement characteristics of the microcapsules were obtained. The average modulus of elasticity was found to be 633 MPa. The self-healing efficiency of the optimized microcapsules was evaluated by means of compressive strength tests. The incorporation of microcapsules reduced the compressive strength of fiber-reinforced mortar by 12–22%. However, it was observed that the microcapsules enhanced the self-healing capacity (recovery in compressive strength) of the mortar.

1. Introduction

Capsule-based self-healing is an approach in which a healing agent is surrounded and protected by a shell material. Upon crack formation, the capsule breaks down and the healing agent releases into the crack. In the 1990s, the first applications of cylindrical capsules in cementitious composites were investigated within a number of studies [1,2]. The capsules can be cylindrical (hollow pipettes or tubes) or spherically made with various range of materials such as glass, polymers, and even lightweight porous aggregates [3–8]. Choi et al. [6] have encapsulated cement powder in a cement-based capsule and used in a mortar mixture to confirm their method. In the study carried out by Sisomphon et al. [9], expanded clay aggregates were impregnated by sodium monofluorophosphate solution which were then coated by cement powder. The clay aggregates were used in ground granulated blast-furnace slag bearing mortars as a self-healing system. Alghamri et al. [10] have also used lightweight aggregates as the host for sodium silicate.

In the past two decades, microcapsules have gained a considerable amount of interest in a diverse spectrum of applications [11]. Various types of microcapsules are being used in many industries such as pharmaceutical, medical, food, cosmetic, textile, paint, and construction [12]. Boh and Šumiga [13] emphasized that various types of microcapsules were used for a wide range of purposes in building/construction materials production and design. Using microcapsules as a self-healing method in engineering materials is one of the most noteworthy applications of them. For the first time, White et al. [14] have proposed the methodology of using microcapsule based self-healing for polymer composites. Since 2001, hundreds of studies have been carried out all over the world to develop the microcapsule based self-healing system in a various range of engineering materials especially polymer-based composites. Microcapsule based self-healing approach in cement-based composites is a relatively new topic as compared to the polymer composites. Before 2011, there were few studies [15,16] that have dealt with microcapsule based self-healing method in

---

cement-based composites. Since the cementitious materials have completely different natures, most of the microcapsules developed for polymer composites cannot provide effective self-healing properties in cement-based composites. It should be noted that the bacteria-based self-healing approach was much more popular as compared with microcapsule based self-healing [17].

Yang et al. [18] have encapsulated methyl methacrylate monomer and triethylborane as the healing agent and the catalyst through an interfacial self-assembly process. The shell of these microcapsules was a silica-based material obtained from a sol-gel reaction. Yang et al. [18] have reported a significant degree of self-healing in the preloaded cementitious specimens. It was also stated that the silica-based shell of microcapsules forms a stronger bond with the cementitious matrix. The shell can chemically and physically be bonded to the matrix, allowing the microcapsule to remain stable for years without deterioration. It is obvious that the adherence between the shell and the matrix must be strong. If the wall-matrix bond strength is low, the crack will advance along with the interface and the microcapsule will not break [19]. Perez et al. [20] have synthesized a new type of microcapsules with a silica-based shell for self-healing in cement-based composites. They have encapsulated Epothin® (epoxy compound) as a healing agent through a sol-gel reaction. The self-healing efficiency of these microcapsules was investigated in their other studies [21,22]. Calvo et al. [22] have reported that although the silica/epoxy microcapsules are well integrated in the matrix, they can lead to a poor mechanical performance of cementitious composite. Dong et al. [23] and Gilford et al. [24] have encapsulated, respectively, epoxy resin E−51 and dicyclopentadiene monomer healing agents with urea–formaldehyde polymer (shell material). Dicyclopentadiene, as healing agent for cementitious materials, was also encapsulated within phenol-formaldehyde resin shell in the scope of the study carried out by Lv et al. [25]. They put the microcapsules into simulated concrete pore solution and cement paste samples to examine the stability performance of the microcapsules. Their test results revealed that the microcapsules have superior stability performance in the simulated pore solution as well as in the real cement environment [25].

All of the above mentioned healing agents can only react with a second component (microencapsulated) or catalyst embedded in cementitious matrices. In two-component agents, the ratio of the first component to the second is usually uncontrolled. Especially for epoxy resins, this ratio is an important factor for complete polymerization. Therefore, single component agents can be considered more appropriate because they can function alone. In recent years, a few studies have dealt with incorporating silica-based microcapsules, as SiO_2 source, in cement-based composites [11,26–31]. Colloidal silica was used as a healing agent/SiO_2 source in polyurethane microcapsules [27]. Besides, Kanellopoulos et al. [11] have encapsulated sodium silicate (SS) solution in gelatin/acacia gum microcapsules through a complex coacervation technique. Giannaros et al. [29] have used two different kinds of microcapsules with a solid (mean size of 130 μm) and a liquid (mean size of 500 μm) core SS. The shell materials of these microcapsules were poly-urea and gelatin-gum Arabic, respectively. Giannaros et al. [29] have reported that incorporating of 4% the SS-containing microcapsules could reduce sorptivity values of damaged specimens after a 28-day healing period. They concluded that the efficacy of the microcapsules in terms of closing cracks and providing sealing was quantified.

Pelletier et al. [26] have introduced the idea of encapsulation of aqueous SS solution in polyurethane microcapsules through interfacial polymerization. The selection of an appropriate production method or technology depends mostly on the properties of core materials. Kanellopoulos et al. [11] has listed these properties as follows: "the cargo material state (liquid or solid), type (organic or inorganic), miscibility as well as its chemical compatibility with the shell materials" ([11] page 2).

In our previous study [31], the sodium silicate/polyurethane microcapsules were synthesized using various amounts of shell-forming

Table 1
The stirring procedures performed in each experiment.

Experiment Code	SS-E (rpm)	SS-FPM (rpm)	SS-P (rpm)	Description
Control	1000	900	800	Same speeds with previous studies [30,31].
EP1	800	700	600	Reduced speeds.
EP2	700	600	500	Reduced speeds.
EP3	500	400	300	Too low PE speed. Experiment was failed
EP4	600	600	600	Constant speed.
EP5	500	500	500	Constant speed.
EP6	600	600	800	Higher and constant ES and SSFPM speeds
EP7	600	500	500	Lower and constant SSFPM and PE speeds
EP8	600	700	700	Higher and constant SSFPM and PE speeds

monomer (MDI). The synthesized microcapsules were characterized in detail through the yield (microencapsulation efficiency), SEM, EDS, FTIR, TGA, and XRD analyses. In another study [30], the components of the core material of those microcapsules, the SS and deionized water, were optimized through the yield and SEM analyses. In this study, the stirring speeds during the synthesizing process were optimized. It is a well-known fact that the diameter of microcapsules can be modified by controlling the stirring speeds as well as altering the synthesizing process. As discussed in the previous study [31] the average diameter of optimized microcapsules (MDI-2) was 29 μm. In this study, it was aimed to increase the average diameter of the microcapsules without causing major problems on the other properties (yield values, wall-thickness, etc.) of the microcapsules. Larger microcapsules can carry larger quantities of core content (healing agent); therefore, they provide increased healing efficiency as compared to smaller microcapsules [32,33]. Besides, the self-healing efficiency of the optimized microcapsules was evaluated by means of a compressive strength test.

2. Experimental program

2.1. Microencapsulation

The encapsulation procedure of the MDI-2 [31] and SS/W-50 [30] microcapsules (shell-forming monomer to core material ratio of 0.67 and SS to water ratio of 0.5) was used as the control procedure in this study. This microencapsulation process has two main steps as follows: 1) dispersion of the aqueous solution of SS in the organic phase, 2) addition of shell-forming solution. Three solutions were prepared in the synthesis process as follows: 1) S1 is a solution of surfactants in toluene, 2) S2 is a solution of shell-forming substances in a certain amount of S1 and toluene, 3) S3 is a solution of SS in deionized water, called core material. The S3 was emulsified in the S1 solution for 20 min (emulsification). After the dispersion and stabilization of aqueous SS microdroplets in the organic phase, the S2 solution was added to the primary emulsion. The mixture was stirred for 20 min at room temperature to form the primary membrane. Then, the temperature was gradually increased to 63 °C, while the stirring speed was reduced. The stirring was continued at 63 °C for 4 h to grow the membrane (polymerization). The microcapsules were vacuum filtered, and then washed with toluene for removal of MDI residue and ethanol/water for removal of surfactant residue and non-encapsulated SS. The microcapsules were dried at room temperature for 48 h and then weighed for yield calculation. The details of materials and microencapsulation processes were presented in preceding studies [30,31].

To produce more microcapsules in a single batch, the amounts of all materials used in the synthesis process were doubled in this study. Therefore, the syntheses were carried out in 250 mL beaker instead of 100 mL beaker. A magnetic cylindrical stir bar with a 30 mm length was
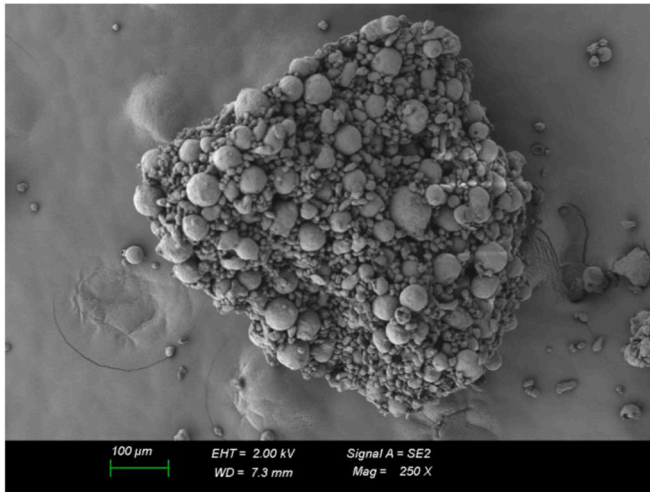
Fig. 1. The aggregation and flocculation of microcapsules synthesized via the EP7 procedures.

Table 2
Properties of the Portland cement used in this study.

Chemical Composition (%)		Physical Properties	
SiO_2	19.1	Specific surface (Blaine) (m^2/kg)	369
Al_2O_3	4.40	Initial setting time (min)	110
Fe_2O_3	3.96	Final setting time (min)	166
CaO	61.85	Volume expansion (mm)	1.00
MgO	2.05		
Na_2O	0.27		
K_2O	0.70	**Compressive Strength**	
SO_3	3.72	2 days (MPa)	27.1
Cl^-	0.0004	7 days (MPa)	43.3
Loss on Ignition	1.82	28 days (MPa)	56.0

Table 3
Mix designs of the OM and MM mixtures (kg/m^3).

	W/C	Water	Cement	Microcapsule	fiber	Aggregate	SP
OM	0.5	250	500	–	143	1372	1
MM	0.5	250	500	25	143	1309	2.5

used for agitation. However, it was observed that this cylindrical stirrer bar was not appropriate for the agitating of the new batch (with doubled materials). In addition, the length of the stirrer bar (30 mm) was not enough due to the higher diameter of the 250 mL beaker. Oval and cylindrical stirrer bars with 30, 35, and 40 mm length were tested for the agitation in this study. The oval one with 40 mm length was the most suitable stirrer bar among the other bars. The mixtures could be homogeneously stirred by the 40 mm oval stirrer bar at even high speeds. It should be noted that the stirring times were kept constant in both previous and present study.

As can be seen in Table 1, based on the preliminary tests, nine different stirring procedures were carried out to obtain optimum stirring speeds. In previous studies, the stirring speed for emulsification (SS-E), stirring speed for the formation of the primary membrane (SS-FPM), and stirring speed for polymerization (SS–P) were 1000 rpm, 900 rpm, and 800 rpm, respectively [30,31]. Therefore, the same procedure was performed in the control experiment. Except for the EP3 experiment, in which the PE was very low (300 rpm), microcapsules formed in all experiments.

2.2. Second washing/drying process of microcapsules

As described in previous studies in detail, after vacuum filtration, sufficient washing, and drying in air, free-flowing powder of microcapsules can be obtained. In other words, the aggregation and flocculation of microcapsules were rarely observed in the optimized microcapsules. However, a certain amount of flocculation can be seen even in well-optimized and washed microcapsules, especially in the doubled materials batches (Fig. 1). The flocculation of microcapsules can lead to an inhomogeneous dispersion of microcapsules in cementitious mixtures. Therefore, the microcapsules were subjected to the second washing/drying process.

To obtain homogeneous and free-flowing powder, the microcapsules synthesized in separate batches were mixed with each other and then, were dispersed in a certain amount of toluene (1000 mL beaker). The slurry of microcapsules was agitated with the magnetic stirrer for 20 min. The microcapsules were vacuum filtered, and then washed with ethanol/water. The wet microcapsules were transferred to watch glasses and then, were dried at room temperature for 48 h.

2.3. Mortars

2.3.1. Materials
CEM I 42.5 R type Portland cement supplied from Denizli Cement

Factory, Turkey was used in the mixtures. The properties of the cement are presented in Table 2. Crushed limestone (0–5 mm) was used as aggregate in mortars. To adjust workability a new generation of Polycarboxylic ether-based superplasticizer (SP) (MasterGlenium® ACE 450) supplied from BASF was used. Besides, straight brass-coated steel micro-fiber with a length of 6 mm, a diameter of 0.16 mm, and tensile strength of 2000 MPa was used as the reinforcement.

2.3.2. Mix designs
For the compressive strength test, two different normal mortar mixtures with a water/cement ratio of 0.5 and a fiber content of 2% by volume were prepared: a mixture without microcapsules called ordinary mortar (OM) and a microcapsule-containing mortar (MM). Microcapsules were used in a concentration of 5% with respect to cement weight (25 kg/m^3). The mix designs of OM and MM mixtures are presented in Table 3. The dosages of water, cement, and microfibers were kept constant in the mixtures. In other words, the required volume for microcapsules was provided by reducing the amount of aggregate. The specific gravity of the microcapsule was considered as 1.00. This assumption was based on the specific gravity of raw materials and the high stability of the water-microcapsules suspension. This assumption in mix design was also checked by comparing the volume and the unit volume weight of the calculated and the real fresh mortar. Furthermore, Kanellopoulos et al. [28] have used a value of ~0.98 g/cm^3 for the density of SS-loaded microcapsules. As expected, the microcapsules have increased the SP demand. The microcapsules are in powder form and the low density of microcapsules leads to a higher quantity of particles in a certain volume; therefore, the specific surface area of the microcapsules is much higher than the aggregate. Consequently, substitution certain amount of aggregate by the microcapsules increases water demand. The required amount of SP was used to achieve a 200 ± 10 mm mini flow table test value (ASTM C1437 [34]).

2.3.3. Preparation of mortars
The optimized microcapsules were dispersed in approximately 90% of the required water for mixtures. The microcapsule/water mixtures were agitated for 10 min by magnetic stirrer until achieving a homogeneous suspension. The microcapsules were successfully suspended in water due to their small size and similar specific gravity with water. This application was done to ensure that the microcapsules remained hydrated and no clusters were formed in the mortar mixture. It should be noted that the dispersion of SS-loading microcapsules in the water is a procedure that can be found in the literature [11]. In addition, this application might lead to a homogeneous dispersion of microcapsule in the cementitious matrix. Half of the required superplasticizer (SP) was
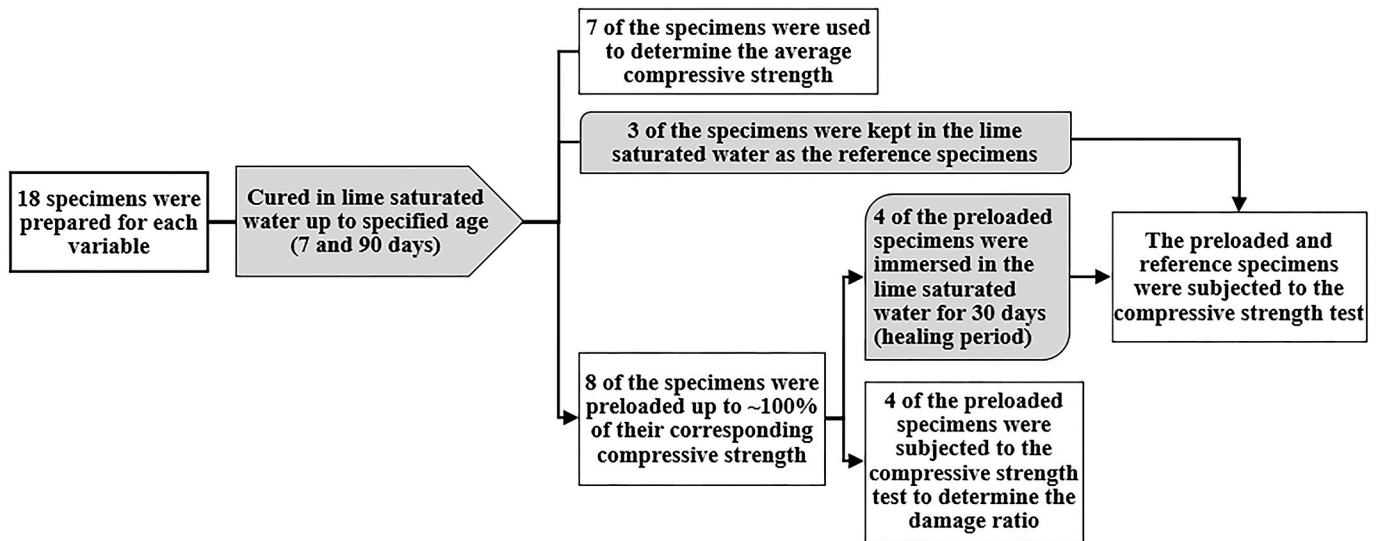
```
┌─────────────────┐   ┌──────────────────┐         ┌─────────────────────────┐
│ 18 specimens    │   │ Cured in lime    │         │ 7 of the specimens were │
│ were prepared   │──▶│ saturated water  │────┬───▶│ used to determine the   │
│ for each        │   │ up to specified  │    │    │ average compressive     │
│ variable        │   │ age (7 and 90    │    │    │ strength                │
└─────────────────┘   │ days)            │    │    └─────────────────────────┘
                      └──────────────────┘    │
```

7 of the specimens were used to determine the average compressive strength

3 of the specimens were kept in the lime saturated water as the reference specimens

Cured in lime saturated water up to specified age (7 and 90 days)

18 specimens were prepared for each variable

4 of the preloaded specimens were immersed in the lime saturated water for 30 days (healing period)

The preloaded and reference specimens were subjected to the compressive strength test

8 of the specimens were preloaded up to ~100% of their corresponding compressive strength

4 of the preloaded specimens were subjected to the compressive strength test to determine the damage ratio

Fig. 2. Flowchart of the compressive strength test procedure.

also added to the water-microcapsule suspension. It was observed that a more homogeneous suspension could be obtained by incorporating superplasticizer into the mixture.

Dry ingredients of the mortar mixtures including fibers were pre-mixed by a Hobart mixer for about 5 min. Then, the microcapsule/water suspension was added to the dry mixture. The remaining water (approximately 10%) was mixed with the remaining SP and then, poured into the mixer. It should be noted that any microcapsules remaining in the suspension beaker were also poured into the mixer using the remaining water and SP.

2.4. Characterization techniques

2.4.1. Scanning electron microscopy and energy-dispersive X-ray spectroscopy

SEM observations of the microcapsules were made by using a scanning electron microscope (Carl Zeiss 300VP, Germany) operated at 2 kV in SE imaging mode. Before SEM imaging, gold sputtering was performed on the samples. Energy dispersive spectrometry (EDS) analyses were conducted with an acceleration voltage of 15 kV.

2.4.2. Optical microscope observations

Optical photomicrographs were acquired by Leica DFC 310FX digital camera mounted on a Leica DM2500P polarized light microscope in plain polarized light mode. Microcapsules were dispersed inside mounting oil (refractive index~1.5) on a glass side. A digital microscope was used to measure the diameter of microcapsules alongside SEM. Upon image acquisition, the diameter of microcapsules was measured on image analysis software.

2.4.3. Nanoindentation test

Continuous stiffness measurement (CSM) which provides continuous measurements of elastic modulus as a function of indentation depth was implemented during the nanoindentation tests. Details about CSM can be found in the previous studies [35,36]. An Agilent Nanoindenter G200 (Keysight, Santa Rosa, CA, USA) equipped with a diamond Berkovich tip was used for nanoindentation. To estimate the elastic modulus of the microcapsule's wall material produced in this study, the nano-indentation test was directly performed on the microcapsule whose diameter was close to the mean diameter of the batch. To be able to glue microcapsules onto the metallic platform separately by avoiding being stacked up on top of each other, microcapsules and the freshly glue-applied metallic platform together were placed in a closed

container then compressed air was applied to introduce turbulence which facilitated precipitation of the microcapsules on the platform evenly. By using this method, it was observed under the microscope that microcapsules could be dispersedly glued on the metallic platform successfully. After solidification of the glue, the metallic platform containing microcapsules was placed into the nanoindenter. An oscillating force with a harmonic displacement of 2 nm at a frequency of 45 Hz was adopted for the CSM method. The surface approach velocity was 10 nm/s. The maximum displacement of 700 nm was applied because the wall thickness was around 3 μm.

2.4.4. Compressive strength

The self-healing mechanism of SS-loaded microcapsules is based on the rupture of their shell during the crack formation in the cementitious matrix, and then the reaction of SS with $Ca(OH)_2$ to form secondary calcium-silicate-hydrate (C–S–H) gel. It is well known that C–S–H is the primary binding phase responsible for the strength in cement-based materials; therefore, in this study, it was aimed to evaluate the contribution of secondary C–S–H in the recovery of compressive strength (RCS). Uniaxial compressive strength tests were conducted by an automatic controlled, 3000 kN capacity hydraulic press machine (ELE Autotest 3000). To assess the self-healing capacity of the mortars in terms of compressive strength, 18 cubic specimens ($50 \times 50 \times 50$ mm) were prepared for each variable. After 7 and 90 days of standard water curing, 15 specimens were taken out form the lime saturated water and left to dry in laboratory air for 1 day. Seven specimens were used to determine the average compressive strength of mixtures. Eight of the specimens were pre-loaded up to ~100% of their corresponding compressive strength. The load was carefully monitored and released at the required predetermined load value (~100%) to avoid further damage. Immediately after preloading, half of the preloaded specimens were subjected to the compressive strength test to determine the damage ratio due to the preloading. The other half of the preloaded specimens (4 specimens) were immersed in the lime saturated water. After 30 days, the preloaded specimens and the remaining specimens from 18 specimens (3 reference specimens – the specimens without preloading) were subjected to the compressive strength test. The flowchart of the compressive strength test procedure is presented in Fig. 2.

It must be noted that a series of specimens were preloaded up to 90% of their corresponding compressive strength. The load was released at the required predetermined load value. Immediately, after preloading, the preloaded specimens were subjected to the compressive strength test to determine the damage ratio due to the preloading. However, there
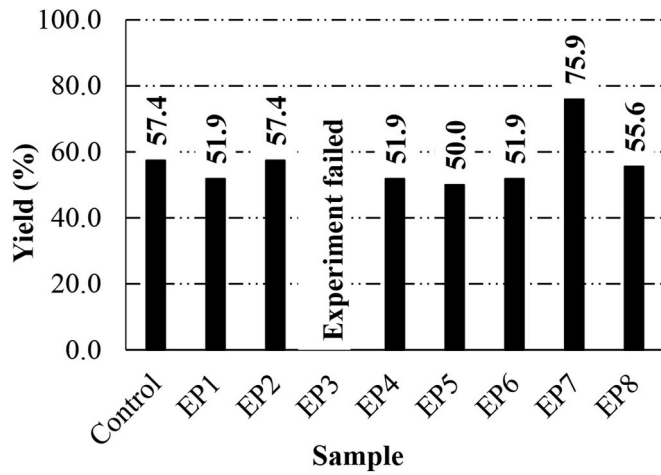
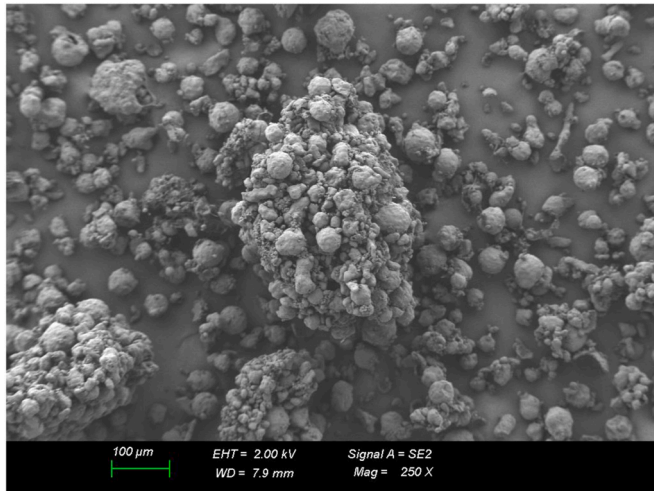**Fig. 3.** Yield values of different synthesizing processes.

Fig. 4. The microcapsules synthesized via the EP6 procedure.

was not any considerable reduction in the compressive strength of specimens. Therefore, in this study, specimens were preloaded up to ~100% of their corresponding compressive strength.

3. Results and discussion

3.1. Optimization of microcapsules

The synthesis was carried out by the emulsification of aqueous SS in toluene using POEDO and Span 85 surfactants and then, followed by interfacial polymerization on the aqueous SS droplets. After vacuum filtration, sufficient washing, and drying in air, free-flowing white powder of microcapsules was obtained. Microencapsulation yields (%) δ given in Fig. 3 were calculated by the following equation [37]:

$$\delta(\%) = \frac{W_M}{W_{HA} + W_{MDI} + W_{SPAN}} \tag{1}$$

where W_M, W_{HA}, W_{MDI}, and W_{Span} are the weights of dried microcapsules powder, healing agent (SS + deionized water), MDI, and Span surfactant, respectively. It should be noted that these yield values include all of the products obtained at the end of the synthesizing process. In other words, the mass of filled, partially-filled, and non-filled microcapsules are included in this calculation. The yield value of microcapsule optimized in previous studies decreased from 85.2% to 57.4%. It is obvious that increasing the amount of the raw materials (doubled) and, as a result, changing the beaker and stirrer bar without modifying the synthesizing process affected adversely the microencapsulation efficiency. The highest yield value (75.9%) was obtained in the EP7 experiment. The yield value is one of the most important criteria that can give an opinion about the efficiency of microencapsulation. Besides, more free-flowing powder of microcapsules was obtained in the EP7 experiment. In other words, the aggregation and flocculation of microcapsules were rarely observed in the EP7 experiment. On the other hand, a large amount of aggregation and flocculation of microcapsules was observed in other samples such as the EP6 and EP8. A typical view of flocculated microcapsules is presented in Fig. 4.

Several SEM-EDS analyses were carried out on the microcapsules. The most well-shaped microcapsules were also observed in the EP7 sample. However, the microcapsules with random shapes can be seen among the spherical microcapsules. For example, the EDS analyses of two microcapsules with spherical and amorphous shapes are presented in Fig. 5. The EDS shows that both of the microcapsules consist of C, O, Na, and Si elements. Therefore, it revealed the existence of polyurethane (shell material) and SS (core material). It should be mentioned that the acceleration voltage of EDS analyses was 15 kV.

In addition, the particles with irregular shapes can be found among the microcapsules. These particles were also observed in previous studies. It can be concluded from EDS analysis that these particles consist mainly of shell-forming material (Fig. 6). Furthermore, Fig. 7 shows the EDS spectra of a cylindrical-like particle and a well-shaped spherical microcapsule. The EDS analysis revealed that the cylindrical-
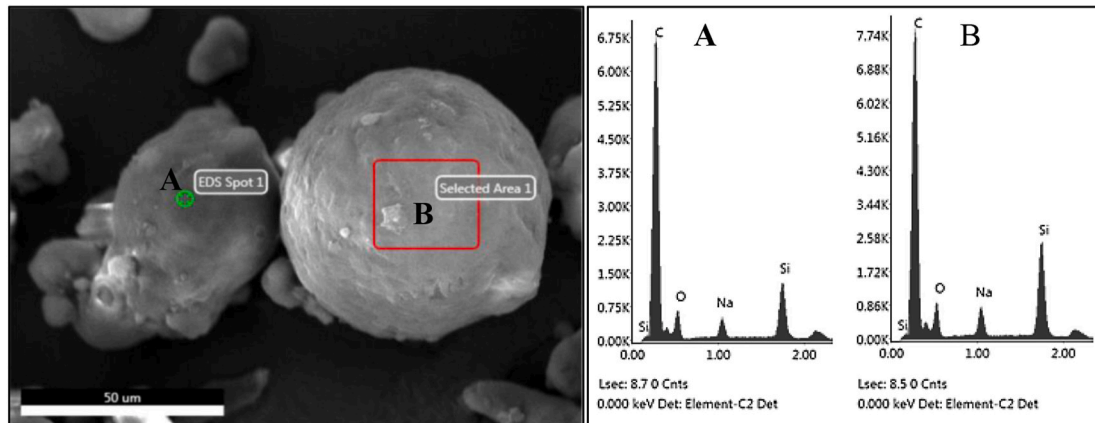

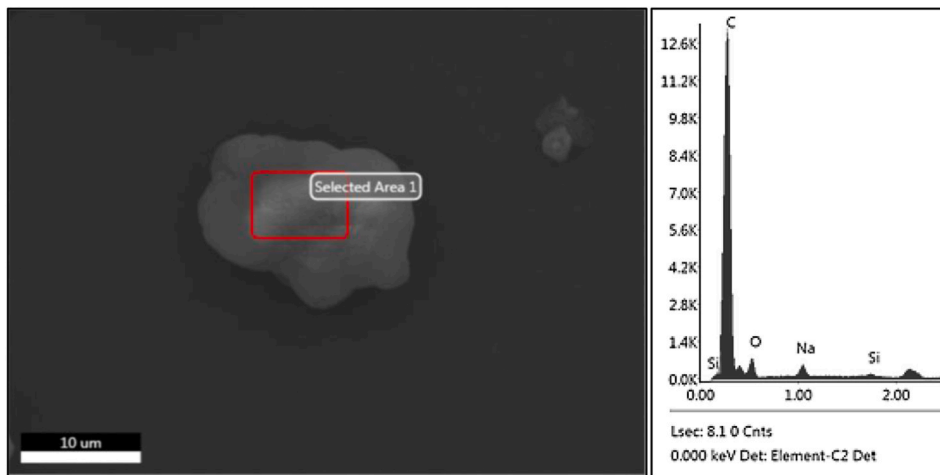**Fig. 5.** The EDS spectra presenting the chemical composition of EP7 microcapsules.

Fig. 6. The EDS spectra presenting the chemical composition of irregular-shaped particles.
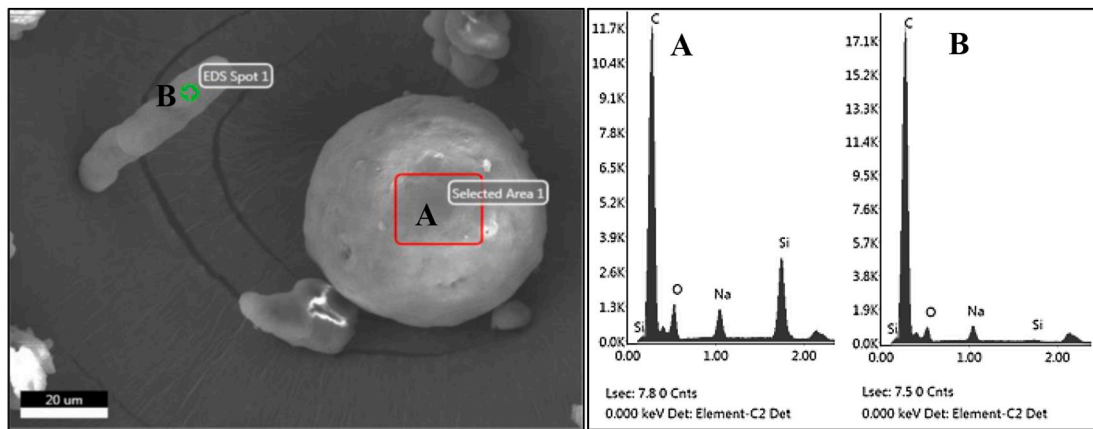

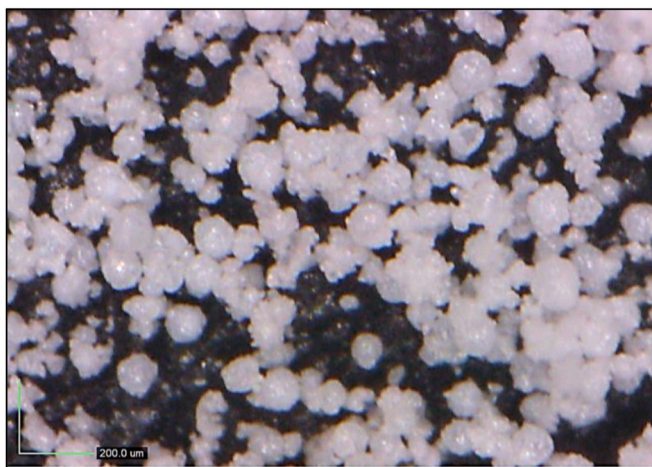**Fig. 7.** The EDS spectra presenting the chemical composition of a cylindrical-like particle.

Fig. 8. A digital photomicrograph of the microcapsules synthesized via the EP7 procedure.
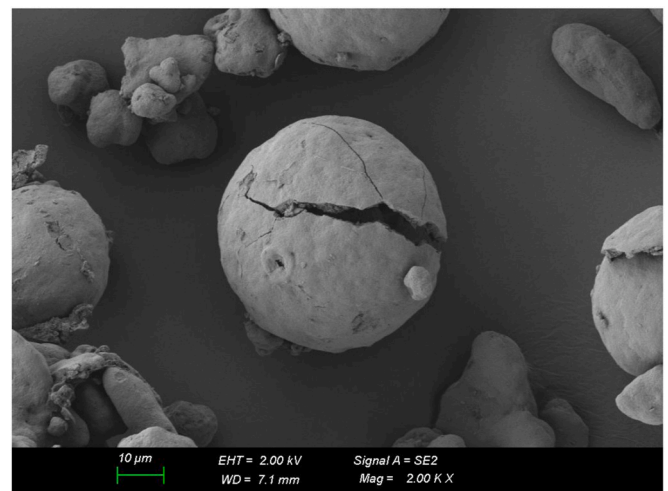

Fig. 9. A fractured microcapsule synthesized via the EP7 procedures.

like particle has also consisted of shell-forming material.

Besides the yield and the morphology of the microcapsules, the average diameter of them was also changed with the new procedure. The average diameters of the microcapsules were obtained by measuring at least 50 microcapsules. The measuring was also carried out on the

digital photomicrographs (Fig. 8). As discussed in the previous study the average diameter of optimized microcapsules (MDI-2) was 29 μm. However, the measurements conducted on the SEM micrograph and digital microscope photomicrographs revealed that the average diameter of the microcapsules synthesized via the EP7 procedures increased
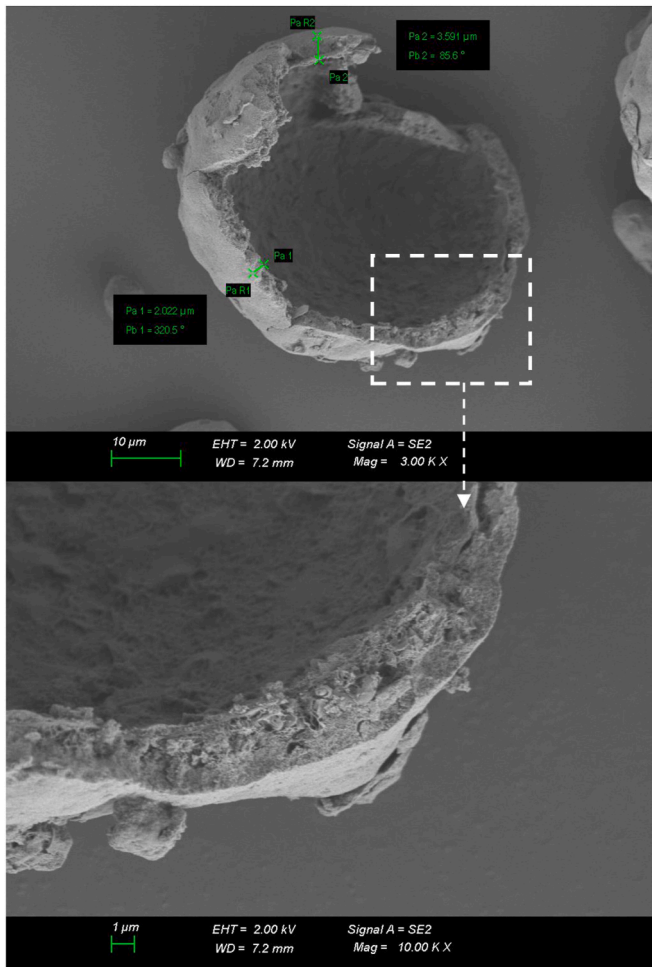
Fig. 10. Cross-section of a fractured microcapsule synthesized via the EP7 procedures.

to 65 μm. It is a well-known fact that the diameter of microcapsules can be increased by decreasing the SS-E [38].

The measurements of the shell thickness of microcapsules were performed on the fractured microcapsules (Fig. 9). The measurements showed that the shell thickness of microcapsules has not changed considerably. It should be noted that the measurements were performed on at least six well-shaped spherical microcapsules (Fig. 10). Similar to

the previous studies, the average shell thickness is 3 μm. In other words, applying different stirring procedures, increasing (doubling) the amounts of raw materials, and using different beaker/stirring bar did not affect the shell thickness of microcapsules remarkably.

As can be seen from the cross-section of the shell, the porosity of the shell is higher near the inner face. Furthermore, it can be seen that the inner face roughness is relatively high. Similar properties were also seen in the microcapsules synthesized in previous studies.

As described earlier a certain amount of flocculation can be seen even in well-optimized and washed microcapsules, especially in the doubled materials batches. Therefore, the EP7 microcapsules were subjected to the second washing/drying process. SEM image and EDS spectrum microcapsule, which was analyzed after the second washing/drying process, are presented in Fig. 11. Similar to the previous sections, the EDS shows that the microcapsules consist of C, O, Na, and Si elements. Therefore, it revealed the existence of polyurethane (shell material) and SS (core material).

The final microcapsules (double-washed EP7 microcapsules) were further characterized by means of optical microscopy and nano-indentation. As can be seen from Fig. 12 the shell material has fawn-beige color in the images. An important percent of microcapsules seems to be empty. The full ones containing SS can be distinguished by their dark color. It should be noted that the sample preparation process could damage the microcapsules. Nevertheless, the yield of the encapsulation method implemented in this study can be enhanced further in the future. The other important finding of optical microscopy is that the average shell thickness measured in SEM images (3 μm) is in concordance with optical microscope images.

Load vs. displacement and modulus of elasticity vs. displacement graphs of the microcapsule that have a diameter around 60 μm, which is close to the mean diameter of the batch, are given in Fig. 13. An average modulus of elasticity was calculated by taking into account the 203 values measured between 550 and 700 nm indentation depths where a plateau was reached. As a result, the average modulus of elasticity was found 633 MPa. It should be noted that the micromechanical properties of microcapsules strongly depend on the capsule diameter [35].

3.2. Evaluation of self-healing efficiency of microcapsules using compressive strength test

Fig. 14 shows the compressive strength test results. It can be seen from test results that the incorporation of microcapsules decreased (12–22%) the compressive strength of mortar. As mentioned earlier the required volume for microcapsules was provided by reducing the amount of aggregate in the mix design. Therefore, it is expected result
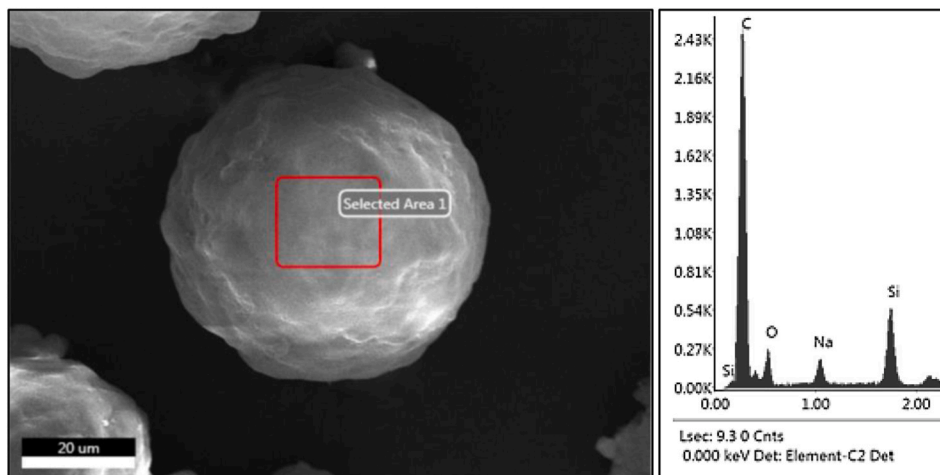

Fig. 11. SEM image and EDS spectrum of a microcapsule (EP7) after the second washing/drying process.
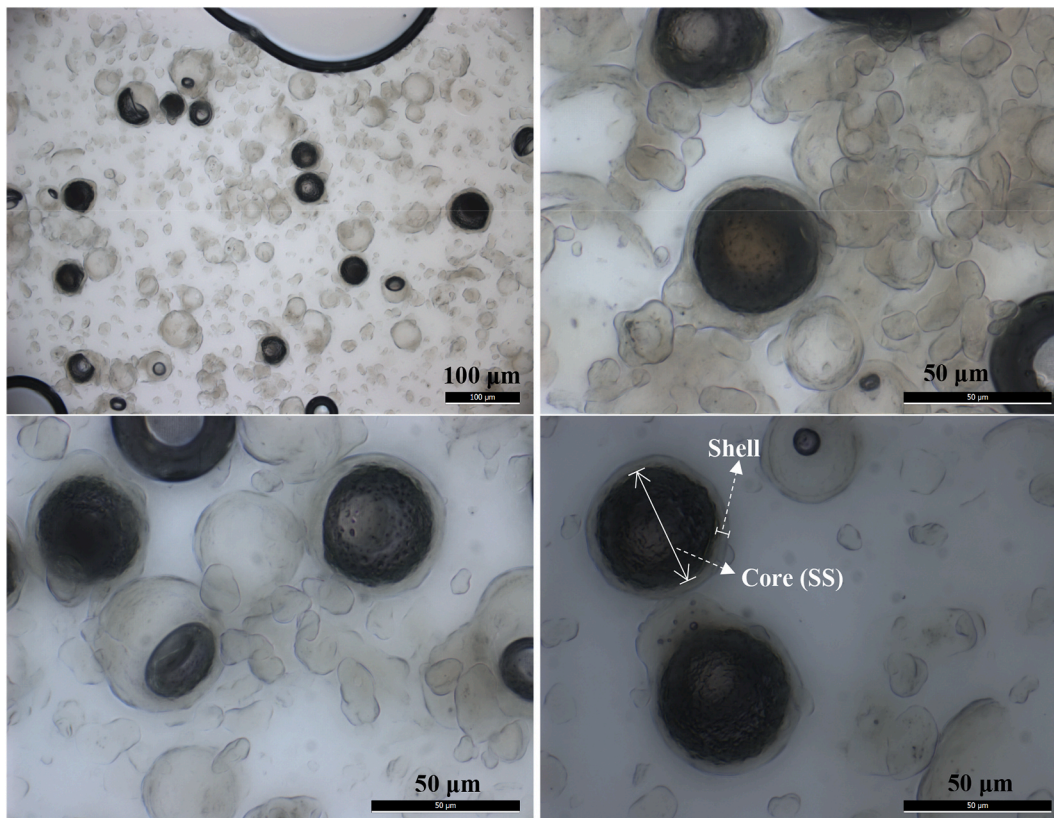
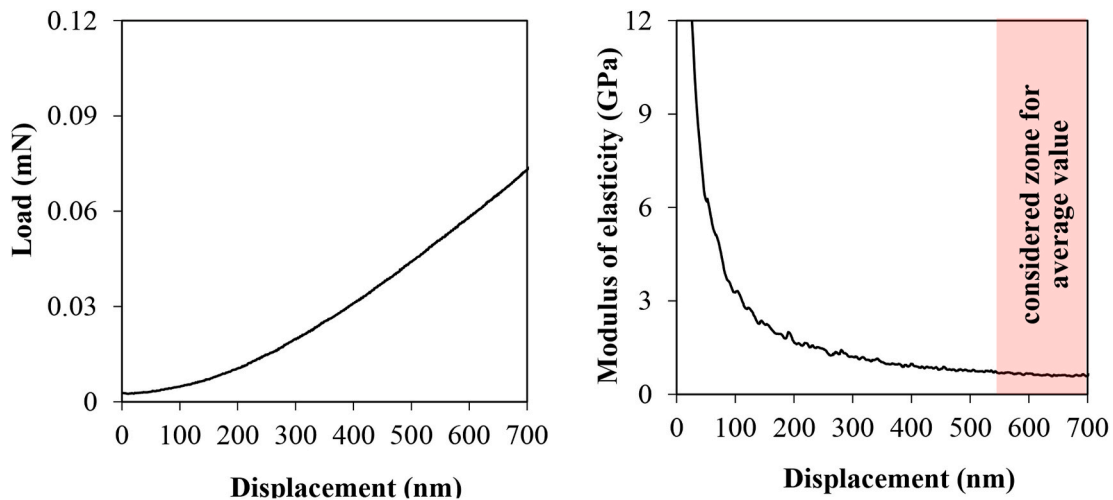**Fig. 12.** Optical photomicrographs of double-washed EP7 microcapsules.

Fig. 13. Load vs. displacement (a) and modulus of elasticity vs. displacement (b) graphs of the microcapsule obtained by nanoindentation.

that replacing a part of such a high strength material (limestone aggregate) with microcapsules that have a lower elastic modulus leads to a decrease in the compressive strength of mortar.

As can be seen from Fig. 15-a, a preloading of up to ~100% of the average strength resulted in a certain extent of damage in the specimens. Despite such a huge preloading level up to ~100% of the average corresponding compressive strength, the reduction in strength did not exceed 20%. It is well-known that plain (without any fiber) concretes or generally cement-based materials are extremely brittle construction material. It has long been recognized that the problem can be mitigated by the incorporating of various types of discontinuous fibers in cementitious matrices.

It is only possible from a correct viewpoint to determine a realistic ratio of self-healing. In this study, the compressive strength of reference specimens and the damage ratios were taken into account in the evaluation of self-healing ratios. The percentages of RCS (self-healing ratios) were expressed by the following equation;

$$\mu(\%) = \frac{c - b}{d - b} \times 100 \qquad (2)$$

where "μ" is the percentage of RCS, "b" and "c" is, respectively, the compressive strengths of preloaded specimens before and after the healing period (30 days), and "d" is the compressive strength of reference specimens after healing period (7 + 30 or 90 + 30 days cured
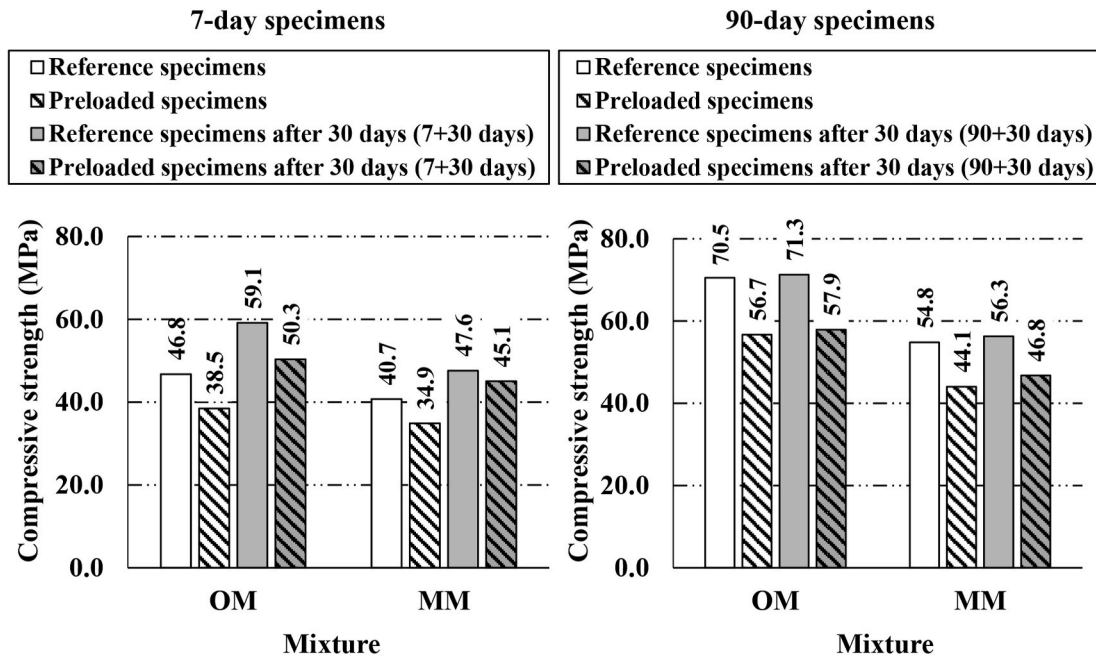
7-day specimens   **90-day specimens**

□Reference specimens
◩Preloaded specimens
▨Reference specimens after 30 days (7+30 days)
◩Preloaded specimens after 30 days (7+30 days)

□Reference specimens
◩Preloaded specimens
▨Reference specimens after 30 days (90+30 days)
◩Preloaded specimens after 30 days (90+30 days)

Fig. 14. The compressive strength test results.
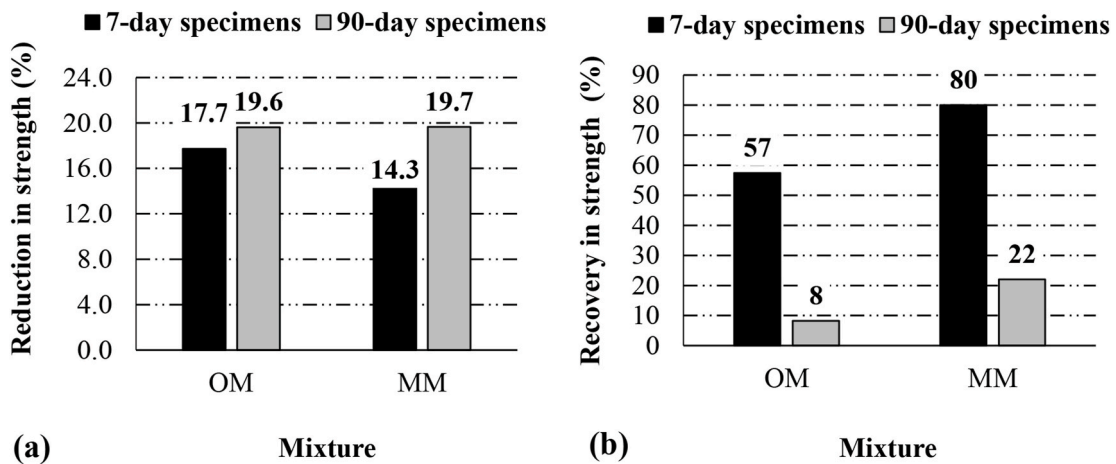

Fig. 15. a) The average reductions in compressive strength of specimens due to preloading. b) The average percentage of RCS.

specimens).

The average percentages of RCS are presented in Fig. 15-b. Despite a preloading up to ~100% of the compressive strength of specimens, a significant ratio of self-healing was detected in the 7-days specimens of both mixtures. Further hydration of unhydrated cement particles (autogenous self-healing phenomenon) is the main reason for the 57% RCS in the OM. On the other hand, incorporating microcapsules increased the RCS percentage up to 80%. In other words, the contribution of SS (the core material) in the reactions on the cracked surfaces is obvious. The reaction between SS and Ca(OH)$_2$ in the case of the presence of water is given as following [10,26,29]:

$$Na_2SiO_3 + Ca(OH)_2 + H_2O \rightarrow x(CaO \cdot SiO_2)H_2O + Na_2O \quad (3)$$
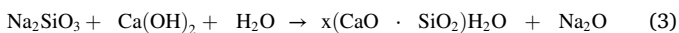
It can be seen that the reaction between calcium hydroxide, a product of cement hydration, and SS can produce secondary C–S–H gel. The specific contribution of microcapsules is more obvious in 90-days cured specimens, in which there are limited unhydrated cement particles. The self-healing efficiency of these microcapsules can be enhanced in the future by further optimization of microencapsulation and

increasing the amount of microcapsule in the mixture. Besides, the survivability of the microcapsules could be affected due to the friction of microcapsules with steel fibers and aggregates during the mixing process. It should be noted that the consistency of the mortar was adequate to decrease that friction. Moreover, the microcapsules have acceptable shell thickness as compared to similar microcapsules previously synthesized in the literature. Detailed investigation and optimization should be carried out regarding the survivability of the microcapsules in mortar and concrete mixtures.

4. Conclusions

Based on the test results of this research, the following conclusions can be drawn:

As expected, modifying the procedure of microencapsulation alters certain properties of microcapsules. Surprisingly, it did not change the shell thickness of microcapsules. In other words, applying different stirring procedures, increasing (doubling) the amount of raw material, and using different beaker/stir bar affected only the yield value and the

average diameter of the microcapsules. It was observed that the second washing of sodium silicate/polyurethane microcapsules is an outstanding approach to obtain a homogeneous powder of microcapsules without any aggregation and flocculation. This powder can be easily dispersed in water to prepare a homogeneous water/microcapsule suspension. The important point is that this suspension can be further homogenized by adding superplasticizer. The average modulus of elasticity, diameter, and shell-thickness of the optimized sodium silicate/polyurethane microcapsules were found 633 MPa, 65 μm, and 3 μm respectively.

Reduction (12–22%) in compressive strength can be evaluated as one of the most problematic side effects of the microcapsule incorporation. This side effect, thus, necessitates further optimization of the mechanical properties of the shell material. It, however, may not be possible to eliminate this side effect completely due to the nature of microcapsules. It was observed that, beyond the autogenous self-healing phenomenon, the microcapsules enhanced the self-healing capacity of the mortar. Nevertheless, further optimization and investigation are necessary to improve the self-healing efficiency of these microcapsules.

Declaration of competing interest

The authors declare that they have no known competing financial interests or personal relationships that could have appeared to influence the work reported in this paper.

Acknowledgments

References

[1] C. Dry, Matrix cracking repair and filling using active and passive modes for smart timed release of chemicals from fibers into cement matrices, Smart Mater. Struct. 3 (2) (1994) 118.

[2] C. Dry, Repair and prevention of damage due to transverse shrinkage cracks in bridge decks, P Soc Photo-Opt Ins 3671 (1999) 253–256.

[3] C. Joseph, A.D. Jefferson, B. Isaacs, R. Lark, D. Gardner, Experimental investigation of adhesive-based self-healing of cementitious materials, Mag. Concr. Res. 62 (11) (2010) 831–843.

[4] T. Nishiwaki, H. Mihashi, B.-K. Jang, K. Miura, Development of self-healing system for concrete with selective heating around crack, J. Adv. Concr. Technol. 4 (2) (2006) 267–275.

[5] V.C. Li, Y.M. Lim, Y.W. Chan, Feasibility study of a passive smart self-healing cementitious composite, Compos. B Eng. 29 (6) (1998) 819–827.

[6] Y.W. Choi, S.R. Oh, B.K. Choi, A study on the manufacturing properties of crack self-healing capsules using cement powder for addition to cement composites, Ann. Mater. Sci. Eng. 2017 (2017) 10, https://doi.org/10.1155/2017/5187543, 5187543.

[7] F.A. Gilabert, K. Van Tittelboom, J. Van Stappen, V. Cnudde, N. De Belie, W. Van Paepegem, Integral procedure to assess crack filling and mechanical contribution of polymer-based healing agent in encapsulation-based self-healing concrete, Cement Concr. Compos. 77 (2017) 68–80.

[8] B. Savija, J. Feiteira, M. Araujo, S. Chatrabhuti, J.M. Raquez, K. Van Tittelboom, E. Gruyaert, N. De Belie, E. Schlangen, Simulation-aided design of tubular polymeric capsules for self-healing concrete, Materials 10 (1) (2017).

[9] K. Sisomphon, O. Copuroglu, A. Fraaij, Application of encapsulated lightweight aggregate impregnated with sodium monofluorophosphate as a self-healing agent in blast furnace slag mortar, Heron 56 (1/2) (2011) 13–32.

[10] R. Alghamri, A. Kanellopoulos, A. A-Tabbaa, Impregnation and encapsulation of lightweight aggregates for self-healing concrete, Construct. Build. Mater. 124 (2016) 910–921.

[11] A. Kanellopoulos, P. Giannaros, D. Palmer, A. Kerr, A. Al-Tabbaa, Polymeric microcapsules with switchable mechanical properties for self-healing concrete: synthesis, characterisation and proof of concept, Smart Mater. Struct. 26 (4) (2017).

[12] M. Singh, K. Hemant, M. Ram, H. Shivakumar, Microencapsulation: a promising technique for controlled drug delivery, Research in pharmaceutical sciences 5 (2) (2010) 65.

[13] B. Boh, B. Šumiga, Microencapsulation technology and its applications in building construction materials Tehnologija mikrokapsuliranja in njena uporaba v gradbenih materialih, RMZ Mater. Geoenviron 55 (3) (2008) 329–344.

[14] S.R. White, N.R. Sottos, P.H. Geubelle, J.S. Moore, M.R. Kessler, S.R. Sriram, E. N. Brown, S. Viswanathan, Autonomic healing of polymer composites, Nature 409 (6822) (2001) 794–797.

[15] Z.X. Yang, J. Holler, X.D. He, X.M. Shi, Laboratory assessment of a self-healing cementitious composite, Transport. Res. Rec. 2142 (2010) 9–17.

[16] F. Xing, Z. Ni, N. Han, B. Dong, X. Du, Z. Huang, M. Zhang, Self-healing Mechanism of a Novel Cementitious Composite Using Microcapsules, 2008. Proceedings of the International Conference on Durability of Concrete Structures, Hangzhou, China.

[17] H.M. Jonkers, A. Thijssen, G. Muyzer, O. Copuroglu, E. Schlangen, Application of bacteria as self-healing agent for the development of sustainable concrete, Ecol. Eng. 36 (2) (2010) 230–235.

[18] Z.X. Yang, J. Hollar, X.D. He, X.M. Shi, A self-healing cementitious composite using oil core/silica gel shell microcapsules, Cement Concr. Compos. 33 (4) (2011) 506–512.

[19] Zhou, S., Zhu, H., Yan, Z., Materials, Theories and Experiments of Microcapsule Self-Healing Method—A Review, Tunneling and Underground Construction2014, pp. 195-204.

[20] G. Perez, E. Erkizia, J.J. Gaitero, I. Kaltzakorta, I. Jimenez, A. Guerrero, Synthesis and characterization of epoxy encapsulating silica microcapsules and amine functionalized silica nanoparticles for development of an innovative self-healing concrete, Mater. Chem. Phys. 165 (2015) 39–48.

[21] G. Perez, J.J. Gaitero, E. Erkizia, I. Jimenez, A. Guerrero, Characterisation of cement pastes with innovative self-healing system based on epoxy-amine adhesive, Cement Concr. Compos. 60 (2015) 55–64.

[22] J.L.G. Calvo, G. Perez, P. Carballosa, E. Erkizia, J.J. Gaitero, A. Guerrero, Development of ultra-high performance concretes with self-healing micro/nano-additions, Construct. Build. Mater. 138 (2017) 306–315.

[23] B.Q. Dong, G.H. Fang, W.J. Ding, Y.Q. Liu, J.C. Zhang, N.X. Han, F. Xing, Self-healing features in cementitious material with urea-formaldehyde/epoxy microcapsules, Construct. Build. Mater. 106 (2016) 608–617.

[24] J. Gilford, M.M. Hassan, T. Rupnow, M. Barbato, A. Okeil, S. Asadi, Dicyclopentadiene and sodium silicate microencapsulation for self-healing of concrete, J. Mater. Civ. Eng. 26 (5) (2014) 886–896.

[25] L. Lv, Z. Yang, G. Chen, G. Zhu, N. Han, E. Schlangen, F. Xing, Synthesis and characterization of a new polymeric microcapsule and feasibility investigation in self-healing cementitious materials, Construct. Build. Mater. 105 (2016) 487–495.

[26] M. Pelletier, R. Brown, A. Shukla, A. Bose, Self-Healing Concrete with a Microencapsulated Healing Agent, 2011. Kingston, USA.

[27] N.P.B. Tan, L.H. Keung, W.H. Choi, W.C. Lam, H.N. Leung, Silica-based self-healing microcapsules for self-repair in concrete, J. Appl. Polym. Sci. 133 (12) (2016).

[28] A. Kanellopoulos, P. Giannaros, A. Al-Tabbaa, The effect of varying volume fraction of microcapsules on fresh, mechanical and self-healing properties of mortars, Construct. Build. Mater. 122 (2016) 577–593.

[29] P. Giannaros, A. Kanellopoulos, A. Al-Tabbaa, Sealing of cracks in cement using microencapsulated sodium silicate, Smart Mater. Struct. 25 (8) (2016).

[30] A. Beglarigale, E. Doğa, Y. Seki, H. Yazici, Optimization of morphology of sodium silicate/polyurethane microcapsules used for self-healing in cementitious materials. 13th International Congress on Advances in Civil Engineering Çeşme/ İzmir, 2018.

[31] A. Beglarigale, Y. Seki, N.Y. Demir, H. Yazici, Sodium silicate/polyurethane microcapsules used for self-healing in cementitious materials: monomer optimization, characterization, and fracture behavior, Construct. Build. Mater. 162 (2018) 57–64.

[32] Z.L. He, S. Jiang, N. An, X.D. Li, Q.F. Li, J.W. Wang, Y.H. Zhao, M.Q. Kang, Self-healing isocyanate microcapsules for efficient restoration of fracture damage of polyurethane and epoxy resins, J. Mater. Sci. 54 (11) (2019) 8262–8275.

[33] J.D. Rule, N.R. Sottos, S.R. White, Effect of microcapsule size on the performance of self-healing polymers, Polymer 48 (12) (2007) 3520–3529.

[34] ASTM C1437-15, Standard Test Method for Flow of Hydraulic Cement Mortar, ASTM International, West Conshohocken, PA, 2015.

[35] B. Savija, H.Z. Zhang, E. Schlangen, Influence of microencapsulated phase change material (PCM) addition on (micro) mechanical properties of cement paste, Materials 10 (8) (2017).

[36] Y.D. Gan, H.Z. Zhang, B. Savija, E. Schlangen, K. van Breugel, Static and fatigue tests on cementitious cantilever beams using nanoindenter, Micromachines-Basel 9 (12) (2018).

[37] D. Saihi, I. Vroman, S. Giraud, S. Bourbigot, Microencapsulation of ammonium phosphate with a polyurethane shell. Part II. Interfacial polymerization technique, React. Funct. Polym. 66 (10) (2006) 1118–1125.

[38] E.N. Brown, M.R. Kessler, N.R. Sottos, S.R. White, In situ poly(urea-formaldehyde) microencapsulation of dicyclopentadiene, J. Microencapsul. 20 (6) (2003) 719–730.